Virologica Sinica 39 (2024) 113–122

Contents lists available at ScienceDirect

Virologica Sinica

journal homepage: www.keaipublishing.com/en/journals/virologica-sinica
www.virosin.org

Research Article

Hsp90 β is critical for the infection of severe fever with thrombocytopenia syndrome virus

Bo Wang [a,b], Leike Zhang [a], Fei Deng [a], Zhihong Hu [a], Manli Wang [a], Jia Liu [a,*]

[a] State Key Laboratory of Virology, Wuhan Institute of Virology, Center for Biosafety Mega-Science, Chinese Academy of Sciences, Wuhan, 430071, China
[b] The Third Affiliated Hospital of Guangzhou Medical University, Guangzhou Medical University, Guangzhou, 511436, China

ARTICLE INFO

Keywords:
Severe fever with thrombocytopenia syndrome virus (SFTSV)
Heat-shock protein 90
Hsp90 β
Host-virus interaction
Nonstructural protein

ABSTRACT

Severe fever with thrombocytopenia syndrome (SFTS) caused by the SFTS virus (SFTSV) is an emerging disease in East Asia with a fatality rate of up to 30%. However, the viral-host interaction of SFTSV remains largely unknown. The heat-shock protein 90 (Hsp90) family consists of highly conserved chaperones that fold and remodel proteins and has a broad impact on the infection of many viruses. Here, we showed that Hsp90 is an important host factor involved in SFTSV infection. Hsp90 inhibitors significantly reduced SFTSV replication, viral protein expression, and the formation of inclusion bodies consisting of nonstructural proteins (NSs). Among viral proteins, NSs appeared to be the most reduced when Hsp90 inhibitors were used, and further analysis showed that their translation was affected. Co-immunoprecipitation of NSs with four isomers of Hsp90 showed that Hsp90 β specifically interacted with them. Knockdown of Hsp90 β expression also inhibited replication of SFTSV. These results suggest that Hsp90 β plays a critical role during SFTSV infection and could be a potential target for the development of drugs against SFTS.

1. Introduction

Severe fever with thrombocytopenia syndrome (SFTS) is an emerging tick-borne disease caused by the SFTS virus (SFTSV). Taxonomically, SFTSV is called *Dabie bandavirus* and belongs to the *Banyangvirus* genus in the *Phenuiviridae* family (Abudurexiti et al., 2019). SFTS is often characterized by acute fever accompanied with thrombocytopenia and leukocytopenia, which can cause bleeding and severe consequences, with a mortality rate as high as 30% (Yu et al., 2011). SFTSV was first identified in China in 2010 and since then has been reported in Japan, South Korea, Myanmar, Vietnam, and Thailand (Gu et al., 2022). SFTS is usually transmitted through tick bites, with the Asian longhorned tick (*Haemaphysalis longicornis*) as the main vector (Tufts et al., 2021; Rochlin et al., 2022). SFTSV can also be transmitted through direct contact with blood and other body fluids of patients (Liu et al., 2012). Although SFTS has been recognized for more than 10 years, little is known about its pathogenic mechanisms, and it remains an important public health issue (Khalil et al., 2021).

The SFTSV genome is composed of three segments of single-stranded, negative-sense RNA, including large (L), middle (M), and small (S) segments. The L segment encodes RNA-dependent RNA polymerase (RdRp) and the M segment encodes two glycoproteins (GPs), Gn and Gc, which form a complex on the surface of virions involved in viral entry and penetration. The S segment applies an ambisense strategy to encode nucleoproteins (NPs) and nonstructural proteins (NSs) (Lam et al., 2013; Albornoz et al., 2016). NSs are virulence factors of SFTSV that interact with several host factors of the interferon (IFN) pathway and suppress the production of antiviral IFN in the host to facilitate viral replication. In addition, NSs promote robust IL-10 expression (Choi et al., 2019), which has been reported to be associated with the severity of SFTS (Song et al., 2018). Therefore, NSs play an important role in the pathogenesis of SFTSV.

Members of the heat-shock protein 90 (Hsp90) family are highly conserved molecules that mainly function as chaperones. In human cells, there are mainly four Hsp90 isomers: Hsp90 α, Hsp90 β, GRP94, and TRAP1. In addition, a truncated isoform (Hsp90 α2) of Hsp90 α also exist (Chen et al., 2005). The Hsp isomers are with different subcellular locations: Hsp90 α and Hsp90 β are located in the cytoplasm (Chen et al., 2005); GRP94 (94-kDa glucose-regulated protein) in the endoplasmic reticulum, and TRAP1 (tumor necrosis factor receptor-associated protein 1) in the mitochondria. Hsp90 plays an essential role in promoting the maturation, folding, assembly, and trafficking of a wide range of cellular

* Corresponding author.
E-mail address: liujia@wh.iov.cn (J. Liu).

https://doi.org/10.1016/j.virs.2023.11.008
Received 21 February 2023; Accepted 22 November 2023
Available online 24 November 2023
1995-820X/© 2023 The Authors. Publishing services by Elsevier B.V. on behalf of KeAi Communications Co. Ltd. This is an open access article under the CC BY-NC-ND license (http://creativecommons.org/licenses/by-nc-nd/4.0/).

proteins, many of which are effectors of key signal transduction pathways controlling cellular processes, such as cell survival, growth, and apoptosis (Hoter et al., 2018). Cancer cells depend on the Hsp90 chaperone machinery for proliferation, and Hsp90 inhibitors have been developed as potential anticancer drugs (Zhang et al., 2022). Moreover, several oncogenic viruses, such as the Epstein-Barr (EBV), hepatitis B, and human papilloma viruses have also been shown to be sensitive to Hsp90 inhibitors (Wang et al., 2017). A compelling body of evidence indicates that Hsp90 is a crucial host factor required for different stages of viral life cycle. For example, Hsp90 is critical for the viral entry of enterovirus 71 and dengue viruses (Reyes-Del Valle et al., 2005; Tsou et al., 2013). Hsp90 regulates viral replication and transcription in influenza and herpes simplex virus infections by participating in correct assembly, functional stabilization, or nuclear import of RNA/DNA-dependent polymerase (Burch and Weller, 2005; Naito et al., 2007). Hsp90 inhibitors lead to the degradation of herpesvirus protein kinase, which is crucial for viral translation (Sun et al., 2013). In addition, Hsp90 is involved in regulation of the immune response induced by viral infections, such as activation of IFN regulatory factors (IRFs), and antigen presentation in response to viral infections. For example, during Sendai virus infections, Hsp90 forms a complex with TBK1-IRF3 that then phosphorylates IRF3 and activates IFN-β induction against viral infection (Yang et al., 2006). Hsp90 can also enhance the response to antigen cross-presentation of lymphocytic choriomeningitis virus nucleoproteins (Basta et al., 2005).

In this study, the role of Hsp90 during SFTSV infection was investigated. We analyzed the effects of Hsp90 inhibitors on viral gene transcription, protein expression, and virion progeny production of SFTSV. The association between NSs and Hsp90 isoforms was also explored. Our data showed Hsp90 β is critical for SFTSV infection and is involved in the formation of NSs inclusion bodies.

2. Materials and methods

2.1. Cells and virus

HEK293, HEK293T, and Vero cells used in this study were obtained from the China Center for General Virus Culture Collection and cultured in Dulbecco's Modified Eagle Medium (Gibco, Waltham, MA, USA) supplemented with 10% fetal bovine serum at 37 °C. The SFTSV WCH strain (Lam et al., 2013) was propagated in Vero cells and viral titer determined using an endpoint dilution assay, as described previously (Zhang et al., 2019).

2.2. Reagents, plasmids, and antibodies

The Hsp90 inhibitors, 17-dimethylaminoethylamino-17-demethoxygeldanamycin (17-DMAG; Cayman Chemical Company, Ann Arbor, MI, USA) and tanespimycin (17-AAG; Cayman Chemical Company), proteasome inhibitor, MG-132 (Beyotime Biotechnology, Shanghai, China), autophagy inhibitor, 3-methyladenine (3-MA; Sigma-Aldrich, St. Louis, MO, USA), lysosome inhibitor, bafilomycin A1 (Baf-A1; MedChemExpress, Monmouth, NJ, USA), and protein synthesis inhibitor, cycloheximide (CHX; MedChemExpress), were dissolved in dimethyl sulfoxide (DMSO) before use.

The pCAGGS-RdRp, pCAGGS-Gn, pCAGGS-NP, and pCAGGS-NSs plasmids used in this study were previously constructed in our laboratory (Zhang et al., 2019). Hemagglutinin (HA)-tagged pCAGGS-HA-NSs and pCAGGS-HA-NP plasmids were constructed by PCR-amplifying the open reading frames of NSs and NP from the pCAGGS-NSs and -NP plasmids using primers with a 5′-HA tag that were then cloned into the pCAGGS vector. pCAGGS-NSs-S-tag was also constructed by the similar method. Human Hsp90 α and β were amplified from the total RNA of HEK293 cells using RT-PCR with the addition of a Flag tag and inserted into the pcDNA3.1 plasmid to obtain pcDNA3.1-Flag-Hsp90 α/β. All plasmids were extracted using a small plasmid extraction kit (Omega Bio-tek, Norcross, GA, USA) according to the manufacturer's instructions.

The homemade rabbit sera anti-NSs, anti-NP, and anti-RdRp, as well as mouse sera anti-NSs and anti-GP (Zhang et al., 2019), were used as primary antibodies to probe the corresponding proteins expressed in HEK293 and HEK293T cells. Mouse anti-β-actin (66009-1-Ig), anti-Hsp90 α (60318-1-Ig), anti-Hsp90 β (67450-1-Ig), anti-GRP94 (60012-2-Ig), and anti-TRAP1 antibodies (67693-1-Ig) used in this study were purchased from ProteinTech (Wuhan, China). Rabbit anti-HA (H6908) and mouse anti-Flag (F1804) antibodies were purchased from Sigma-Aldrich.

2.3. Drug inhibition assays

First, cytotoxicity of the Hsp90 inhibitors, 17-AAG and 17-DMAG, was tested. To this end, 17-AAG (0.5–8 μmol/L) or 17-DMAG (10–640 nmol/L) was added to HEK293 cells for 24 h, and DMSO used as a control. Cytotoxicity was then determined using a cell counting kit-8 (CCK8; Beyotime Biotechnology) according to the manufacturer's protocol. To evaluate antiviral efficiency of the inhibitors, HEK293 cells (2×10^5 cells/well) cultured overnight in 24-well Petri dishes were infected with SFTSV at a multiplicity of infection (MOI) of 1 $TCID_{50}$ (50% tissue culture infectious dose)/cell for 1 h at 37 °C, and the supernatant then replaced with fresh medium containing different concentrations of 17-AAG (0.5–2 μmol/L), 17-DMAG (40–160 nmol/L), or DMSO. At 24 h post-infection, viral titers in the supernatant were determined by an endpoint dilution assay, as described previously (Zhang et al., 2019). Cells were lysed to either quantify the SFTSV genome using quantitative real-time PCR (RT-qPCR) or to detect the expression of SFTSV proteins using Western blotting. The cells were fixed with 4% paraformaldehyde for immunofluorescence staining. A minimum of two experiments were performed.

To detect whether the Hsp90 inhibitor, 17-AAG, suppresses the overexpressed viral proteins, HEK293T cells were transfected with pCAGGS-NSs, pCAGGS-RdRp, pCAGGS-Gn, or pCAGGS-NP plasmids using Lipofectamine 3000 (Invitrogen, Waltham, MA, USA) according to the manufacturer's protocols. At 6 h post-transfection, cells were treated with 2 μmol/L 17-AAG or DMSO for 24 h, and cell lysates thereafter collected for Western blotting analysis.

For the degradation pathway inhibitor assay, HEK293 cells were infected with SFTSV at an MOI of 5 for 24 h. Supernatants were then replaced with fresh medium containing 17-AAG (2 μmol/L) with MG-132 (500 nmol/L), 3-MA (5 μmol/L), or Baf-A1 (100 nmol/L). Fresh medium containing the individual drugs or DMSO were also used as controls. After a 6 h incubation period, the cells were collected and viral proteins detected using Western blotting. For the protein synthesis inhibitor test, HEK293T cells were infected with SFTSV at an MOI of 2 and then treated with 17-AAG (2 μmol/L) and/or CHX (50 μmol/L) at 24 h post-infection. At 12 h post-treatment, cells were collected for Western blotting analyses. Then a parallel assay in transfected cells was also performed. HEK293T cells were transiently transfected with pCAGGS-NP or pCAGGS-NSs-S-tag, and treated with 17-AAG (2 μmol/L) with or without CHX (50 μmol/L) at 6 h post-transfection. The expression levels of NSs and NP were detected by Western blotting analysis at 24 h post-transfection.

2.4. Quantitative real-time PCR

Total cellular mRNA was extracted using the TRIzol reagent (Promega, Madison, WI, USA) according to the supplier's protocol. RNA was converted to cDNA using RT-PCR with Moloney murine leukemia virus reverse transcriptase (Promega). RT-qPCR was performed using specific primers targeting viral genes (L, M, and S segments) with SYBR Premix Ex Taq (Applied Biosystems, Waltham, MA, USA). Gene expression was

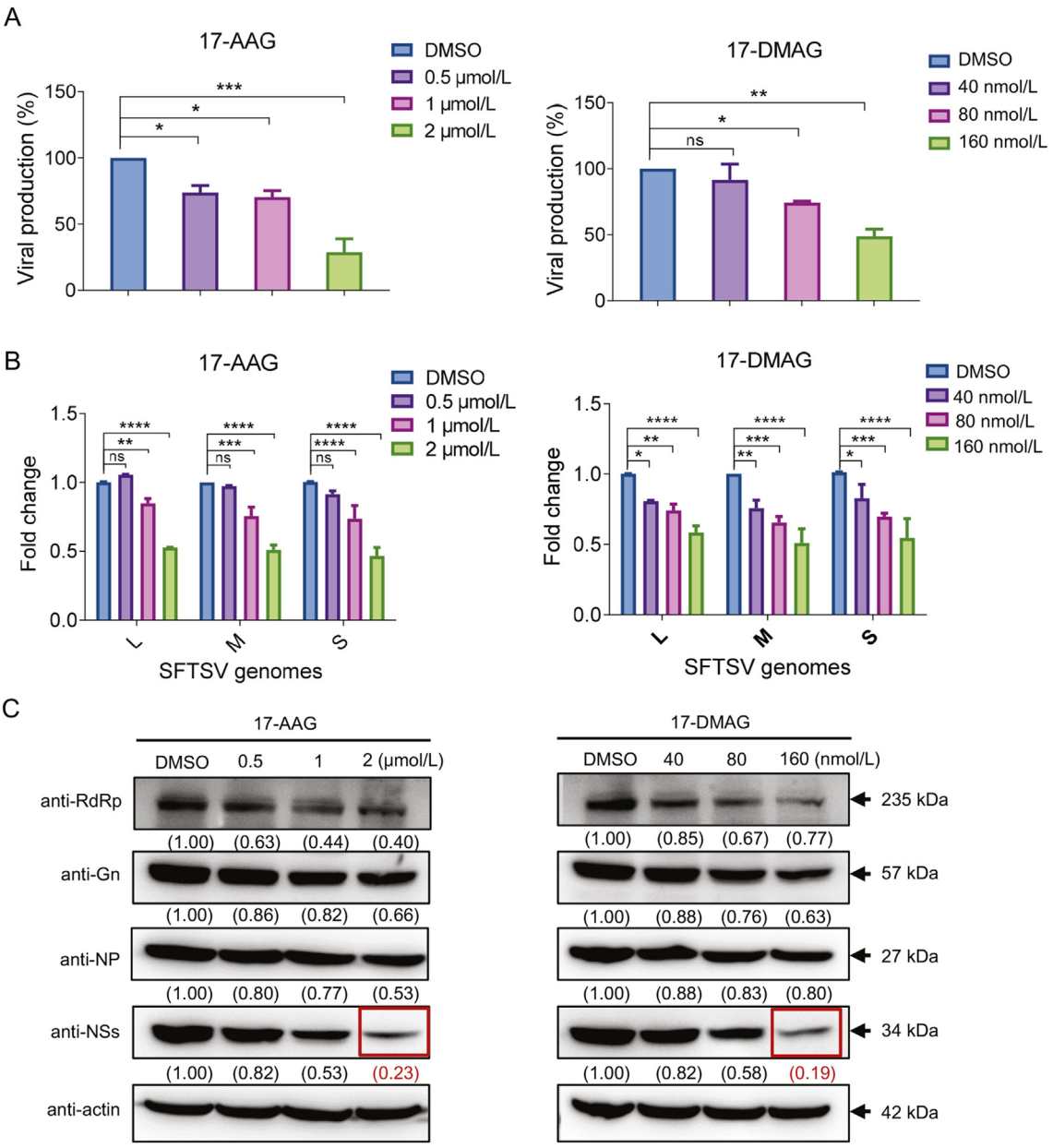

Fig. 1. Heat-shock protein 90 (Hsp90) inhibitors influence severe fever with thrombocytopenia syndrome virus (SFTSV) replication. HEK293 cells were infected with SFTSV at a multiplicity of infection (MOI) of 1 and treated with the indicated drugs or dimethyl sulfoxide (DMSO). At 24 h post-infection, the viral production, genome copy number and viral protein expression level were determined. The viral titers in supernatant were determined using an endpoint dilution assay and normalized to that of DMSO group (**A**). Cells were lysed to either quantify the SFTSV genome using RT-qPCR (**B**) or detect SFTSV protein expression using Western blotting (**C**). For analysis of the viral production and genome replication, three in-dependent experiments were performed. For detection of viral protein expression, two in-dependent experiments were performed, and representative immunoblot results are shown in the figure. Data are shown as the mean ± SD in (**A**) and (**B**). Statistical significance was determined using one-way (**A**) or two-way (**B**) ANOVA followed by Dunnett's multiple comparisons test. ns, not significant; *, $P < 0.05$; **, $P < 0.01$; ***, $P < 0.001$, and ****, $P < 0.0001$.

normalized to that of the housekeeping β-actin gene, as previously described (Zhang et al., 2019).

2.5. Western blotting

Total cellular protein was separated using SDS-PAGE and transferred to a polyvinylidene difluoride membrane (Merck Millipore, Burlington, MA, USA). After blocking with 5% bovine serum albumin (BSA), the membrane was probed with primary antibodies and incubated with horseradish peroxidase-conjugated goat anti-mouse IgG (Sigma-Aldrich, 71045-M) as a secondary antibody. The protein bands were detected using an enhanced chemiluminescence kit (Thermo Fisher Scientific, Waltham, MA, USA). Protein expression levels were assessed using ImageJ software according to the immunoblotting method. The integrated density of viral or host proteins was first normalized to that of β-actin and then compared to that of the control group.

2.6. Immunofluorescence assay

Transfected or infected HEK293 cells were fixed with 4% paraformaldehyde at 4 °C overnight and permeabilized with 0.25% Triton X-100. The cells were then sealed with blocking buffer (PBS containing 5%

BSA) for 2 h, followed by incubation with mouse anti-NSs or rabbit anti-Flag antibodies as the primary antibody at 4 °C overnight. After washing three times with PBS, AF 488/594-conjugated goat anti-mouse or anti-rabbit IgG was added for 1 h at 37 °C as a secondary antibody. Thereafter, nuclei were stained with DAPI (Beyotime Biotechnology) at 25 °C for 10 min. Fluorescence images were captured using a two-photon microscope (A1RMP; Nikon).

2.7. Co-immunoprecipitation

Co-immunoprecipitation (Co-IP) analysis was performed to distinguish the interactions between NSs and Hsp90 isoforms. To analyze the interaction between NSs and endogenous Hsp90 isomers, HEK293T cells were transfected with pCAGGS-HA-NP or pCAGGS-HA-NSs plasmids. To detect the interaction of NSs with exogenous Hsp90 α or β, HEK293T cells were co-transfected with pCAGGS-HA-NSs and pcDNA3.1-Flag-HSP90α or pcDNA3.1-Flag-HSP90β. After 48 h, cells were lysed by lysis buffer (25 mmol/L Tris, pH 7.4, 150 mmol/L NaCl, 1 mmol/L EDTA, 1% TritonX-100, 1 × Roche complete mini-protease inhibitor cocktail) for Co-IP analysis. Briefly, cell lysates were pre-treated with protein A agarose beads (Roche Applied Sciences, Penzberg, Germany) at 4 °C for 1 h. Thereafter, the supernatant was collected after centrifugation at 15,000×*g* for 15 min and incubated with 2 μL anti-HA or anti-Flag antibodies at 4 °C overnight and then incubated with fresh protein A conjugated agarose beads at 4 °C for 3 h. The immunoprecipitate was washed three times with cell lysis buffer, followed by the addition of 30 μL Laemmli sample buffer to elute bound proteins on beads for Western blotting.

2.8. siRNA transfection

HEK293 cells were pre-seeded in 24-well plates at a density of 2×10^5 cells and transfected with 30 pmol *HSP90AB1* siRNA #1 (5′-CGCATGGAAGAAGTCGATTAG-3′) or #2 (5′-CTTGTGTTGAAGGCAGTAAAC-3′) using Lipofectamine 3000 (Invitrogen). In a parallel experiment, a scrambled siRNA was used as a control. All siRNAs were synthesized by GenePharma (Shanghai, China). At 48 h post-transfection, the cells were infected with SFTSV at an MOI of 1 for 48 h. Thereafter, intracellular viral genome, protein level, and supernatant virion progeny production were detected using RT-qPCR, Western blotting, and endpoint dilution assays, respectively.

2.9. Statistical analyses

Statistical analyses were performed using one- or two-way analysis of variance with GraphPad Prism. Statistical significance was set at $P < 0.05$. ns indicates $P > 0.05$, $^*P < 0.05$, $^{**}P < 0.01$, $^{***}P < 0.001$, and $^{****}P < 0.0001$.

3. Results

3.1. Inhibition of Hsp90 reduces SFTSV infection

To assess the effects of Hsp90 inhibition on SFTSV infection, two well-known Hsp90 inhibitors, 17-AAG and 17-DMAG, were used. Both drugs are geldanamycin analogs that target the N-terminal ATP-binding domain of Hsp90 and inhibit its chaperone activity (Solit and Chiosis, 2008). First, the cytotoxicity of 17-AAG and 17-DMAG in HEK293 cells was measured using the CCK-8 assay. 17-AAG and 17-DMAG showed no obvious cytotoxicity at concentrations of ≤2 μmol/L and ≤160 nmol/L, respectively (Supplementary Fig. S1). Therefore, 17-AAG (0.5–2 μmol/L) and 17-DMAG (40–160 nmol/L) were selected to treat the SFTSV-infected HEK293 cells, and DMSO was used as a control. At 24 h post-infection, the viral yield in the supernatant, as well as the viral genome and protein in the cell, were detected. As shown in Fig. 1A, both 17-AAG and 17-DMAG reduced SFTSV infectivity in a dose-dependent manner. Consistently, viral genomic replication was reduced by both inhibitors, and the inhibition efficiencies of the three genome fragments

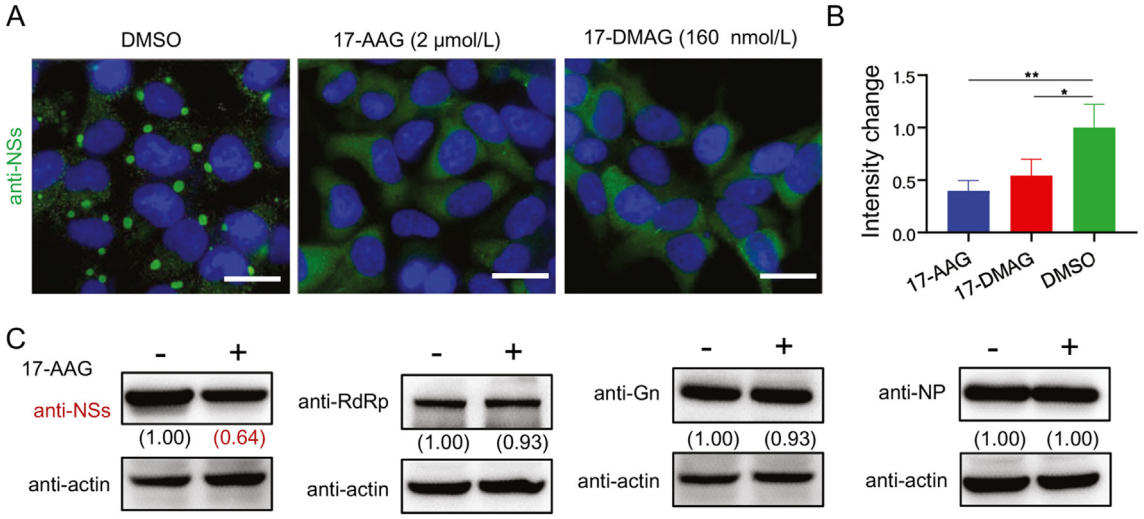

Fig. 2. Nonstructural proteins (NSs) are affected by Hsp90 inhibitors. **A** 17-AAG and 17-DMAG inhibit the formation of inclusion bodies induced by NSs. SFTSV-infected HEK293 cells were treated with 17-AAG or 17-DMAG for 24 h and then stained using anti-NSs antibodies for immunofluorescence analysis. Infected cells treated with DMSO were used as controls and nuclei stained with DAPI. Scale bars, 20 μm. **B** The fluorescence intensity analysis of the NSs protein in Fig. 2A. The mean fluorescence intensity of the NSs protein was calculated through ImageJ software, and the intensity change was obtained as the fluorescence intensity in 17-AAG/17-DMAG treated group normalized to DMSO group. Two independent experiments were performed. Data are shown as the mean ± SD (n > 20 cells). Statistical significance was determined using one-way ANOVA followed by Dunnett's multiple comparisons test. $^*P < 0.05$ and $^{**}P < 0.01$. **C** Hsp90 inhibitors specifically suppressed the overexpression of NSs. HEK293T cells were transfected with plasmids expressing NSs, RNA-dependent RNA polymerase (RdRp), Gn, or nucleoproteins (NPs), respectively. At 6 h post-transfection, the cells were treated with 2 μmol/L 17-AAG for another 24 h. Thereafter, the cell lysates were subjected to Western blotting analysis with anti-NSs, anti-NP, anti-Gn, and anti-RdRp antibodies. The relative levels of viral and host proteins were assessed using ImageJ software according to the immunoblot and showed under the corresponding image. Two independent experiments were performed, and representative results are shown in the figure.

(L, M, and S) appeared to be similar (Fig. 1B). Western blotting analysis showed that the Hsp90 inhibitors also decreased expression levels of all detected viral proteins (Fig. 1C). At the highest drug concentration, expression of NSs was most obviously affected (Fig. 1C, red box) in comparison to that of RdRp, Gn, and NP. These results indicated that Hsp90 plays an important role in SFTSV infection.

3.2. Nonstructural proteins are one of the main targets of Hsp90 inhibitors

During SFTSV infection, NSs can form cytoplasmic inclusion bodies that function as antagonists of antiviral IFN-α/β (Khalil et al., 2021). As NSs appeared to be the viral proteins most obviously affected by Hsp90 inhibitors (Fig. 1C), we then examined whether the formation of inclusion bodies was also affected. HEK293 cells were infected with SFTSV at an MOI of 1 and treated with Hsp90 inhibitors; at 24 h post infection, the cells were stained for immunofluorescence assays using anti-NSs antibodies. As shown in Fig. 2A, no NSs inclusion bodies were observed in the 17-AAG- or 17-DMAG-treated infected cells, whereas many inclusion bodies were formed in the DMSO-treated infected cells. We also measured the fluorescence intensity of NSs, as shown in Fig. 2B, the mean fluorescence intensity of NSs protein in 17-AAG and 17-DMAG treated cells were about 40% and 54% of that of the DMSO group. These result showed that the Hsp90 inhibitors decreased expression levels of NSs and disrupted the formation of NSs inclusion bodies.

To further confirm that Hsp90 inhibitors specifically target NSs, 17-AAG was added to HEK293T cells that were transiently transfected with plasmids individually expressing NSs, RdRp, Gn, or NP. Western blotting analysis showed that among the four viral proteins, only expression of NSs was decreased by 17-AAG treatment (Fig. 2C). Therefore, we speculated that the influence of Hsp90 inhibitors on the other viral proteins during SFTSV infection (Fig. 1C) might be due to the secondary effects of NS reduction on viral replication. We also detected the impact of 17-AAG on viral gene transcription. At 24 h post-infection, the SFTSV-infected cells were treated with 17-AAG for 6 h, then the viral

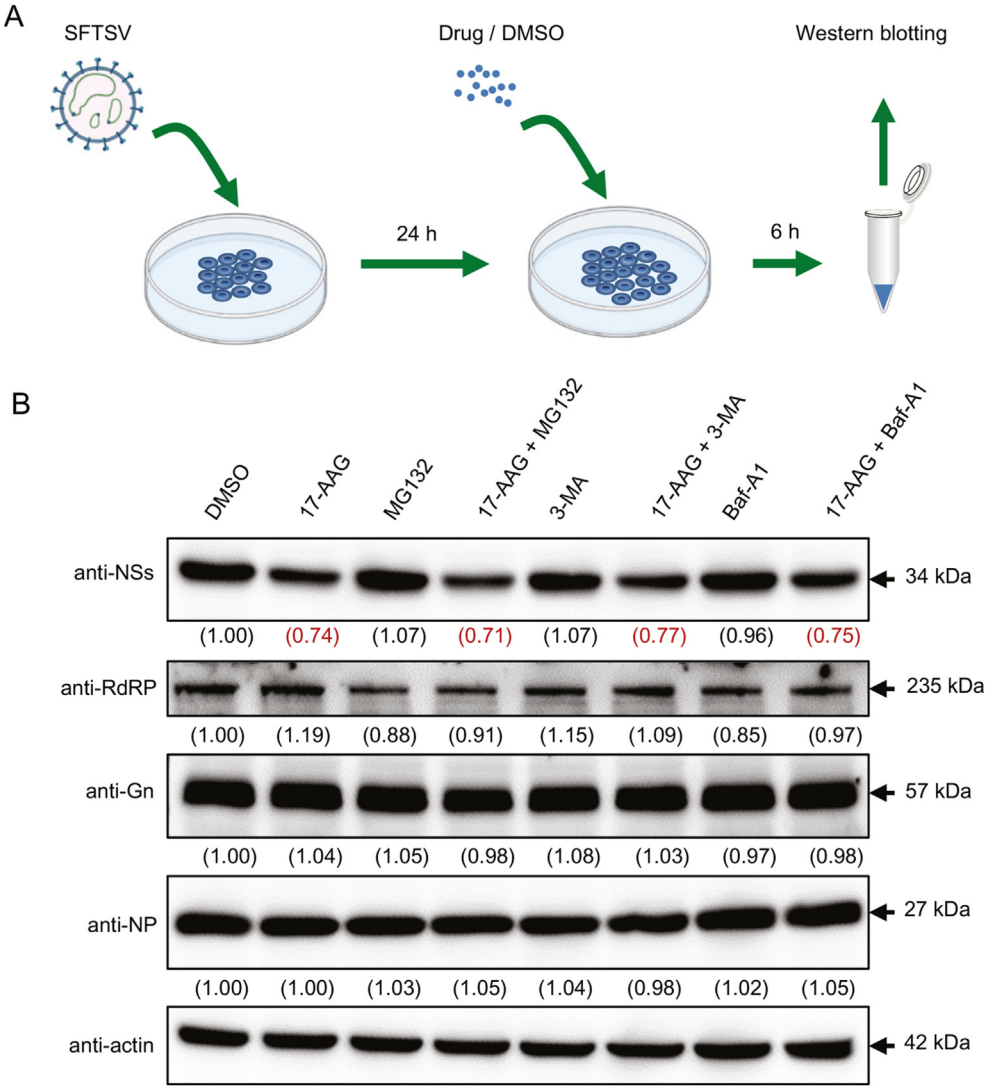

Fig. 3. Suppression of protein degradation pathways could not recover the reduced expression of NSs caused by the Hsp90 inhibitor, 17-AAG. **A** Workflow of the experiment. HEK293 cells were infected with SFTSV with an MOI of 5 for 24 h, thereafter the supernatants were replaced with fresh medium containing 17-AAG (2 μmol/L), MG-132 (500 nmol/L), 3-methyladenine (3-MA; 5 μmol/L), and bafilomycin A1 (Baf-A1; 100 nmol/L), individually or in combination, for 6 h. Fresh medium containing DMSO was used as a control. Then, viral proteins were detected using Western blotting with anti-NSs, anti-RdRp, anti-Gn, anti-NP, and anti-β-actin antibodies. **B** Results of the Western blotting analyses. The relative levels of viral and host proteins were assessed using ImageJ software according to the immunoblot and showed under the corresponding image. Two independent experiments were performed, and representative results are shown in the figure.

protein and mRNA of viral genes were detected. As shown in Supplementary Fig. S2, 17-AAG only reduced protein level of NSs and had no effect on other viral proteins, while the transcription of all viral genes were not affected. This indicated that the down-regulation of NSs protein was at post-transcription level.

3.3. Reduced nonstructural protein levels were likely not due to protein degradation

Hsp90 belongs to a family of molecular chaperones that facilitate proper protein folding, stability, interactions, and intracellular trafficking. In the absence of Hsp90, many unfolded or misfolded Hsp90 client proteins are degraded via proteasome–ubiquitin or autophagy pathways (Chen et al., 2012). Therefore, we investigated whether the downregulation of NSs expression caused by 17-AAG was dependent on intracellular protein degradation pathways. To this end, SFTSV-infected cells were treated with 17-AAG and/or the proteasome (MG-132), autophagosome (3-MA), and lysosome (Baf-A1) inhibitors at 24 h post-infection for 6 h. The expression of viral proteins was then analyzed using Western blotting (Fig. 3A). As shown in Fig. 3B, except for that of NSs, the expression levels of other viral proteins were not distinctly influenced by drug treatments. The expression level of NSs was reduced when 17-AAG was added alone or co-administered with MG-132, 3-MA, or Baf-A1. This suggests that protein degradation pathway inhibitors could not reverse the decrease in expression of NSs induced by 17-AAG, and that this decrease might not be due to protein degradation.

3.4. Hsp90 inhibitor, 17-AAG, likely affects the synthesis of nonstructural proteins

We then tested whether Hsp90 inhibitors affected protein synthesis of NSs. HEK293T cells were infected with SFTSV at an MOI of 2. At 24 h post-infection, the supernatant of the infected cells was replaced with fresh media containing 17-AAG with or without the protein synthesis inhibitor, CHX. Changes in viral protein expression levels of NSs and NP at 12 h post-treatment were detected using Western blotting and shown in Fig. 4A. For NSs, when 17-AAG was added alone, consistent with the results shown in Fig. 1, protein expression levels of NSs were reduced. And the degree of NSs protein that changed after treatment with 17-AAG alone was similar to that of CHX alone. When co-application of 17-AAG with CHX, slight synergy effect was observed in reduction of NSs. While for NP, protein expression levels of NP was not effect by treatment with 17-AAG alone, but obviously decreased by CHX without or with 17-AAG compared to the DMSO group. Furthermore, we conducted a parallel assay in transfected cells (Fig. 4B). 17-AAG with or without CHX was added to HEK293T cells that were transiently transfected with plasmids individually expressing NSs or NP at 6 h post-transfection. Western

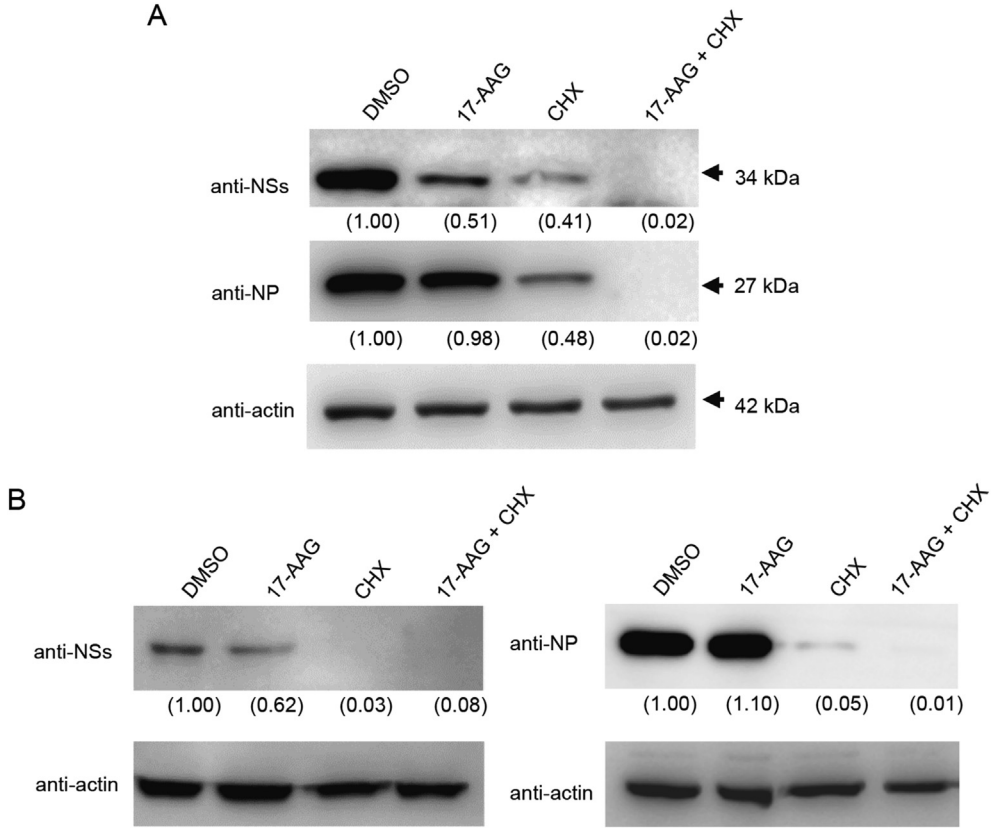

Fig. 4. Hsp90 inhibitor, 17-AAG, likely affects the protein synthesis of NSs. **A** 17-AAG inhibited the protein synthesis of NSs in infected cells. HEK293T cells were infected with SFTSV at an MOI of 2 for 24 h. Then, the supernatants were replaced with fresh medium containing 17-AAG (2 μmol/L), and/or cycloheximide (CHX; 50 μmol/L). Fresh medium containing DMSO was used as a control. The cells were harvested at 12 h post-treatment for Western blotting analysis. Two independent experiments were performed, and representative results are shown in figure. **B** 17-AAG effected the protein synthesis of NSs in transfected cells. HEK293T cells were transfected with plasmids expressing NSs or nucleoproteins (NPs), respectively. At 6 h post-transfection, the cells were treated with 2 μmol/L 17-AAG, and/or cycloheximide (CHX; 50 μmol/L) for another 24 h. Thereafter, the cell lysates were subjected to Western blotting analysis. The relative levels of viral and host proteins were assessed using ImageJ software according to the immunoblot and showed under the corresponding image.

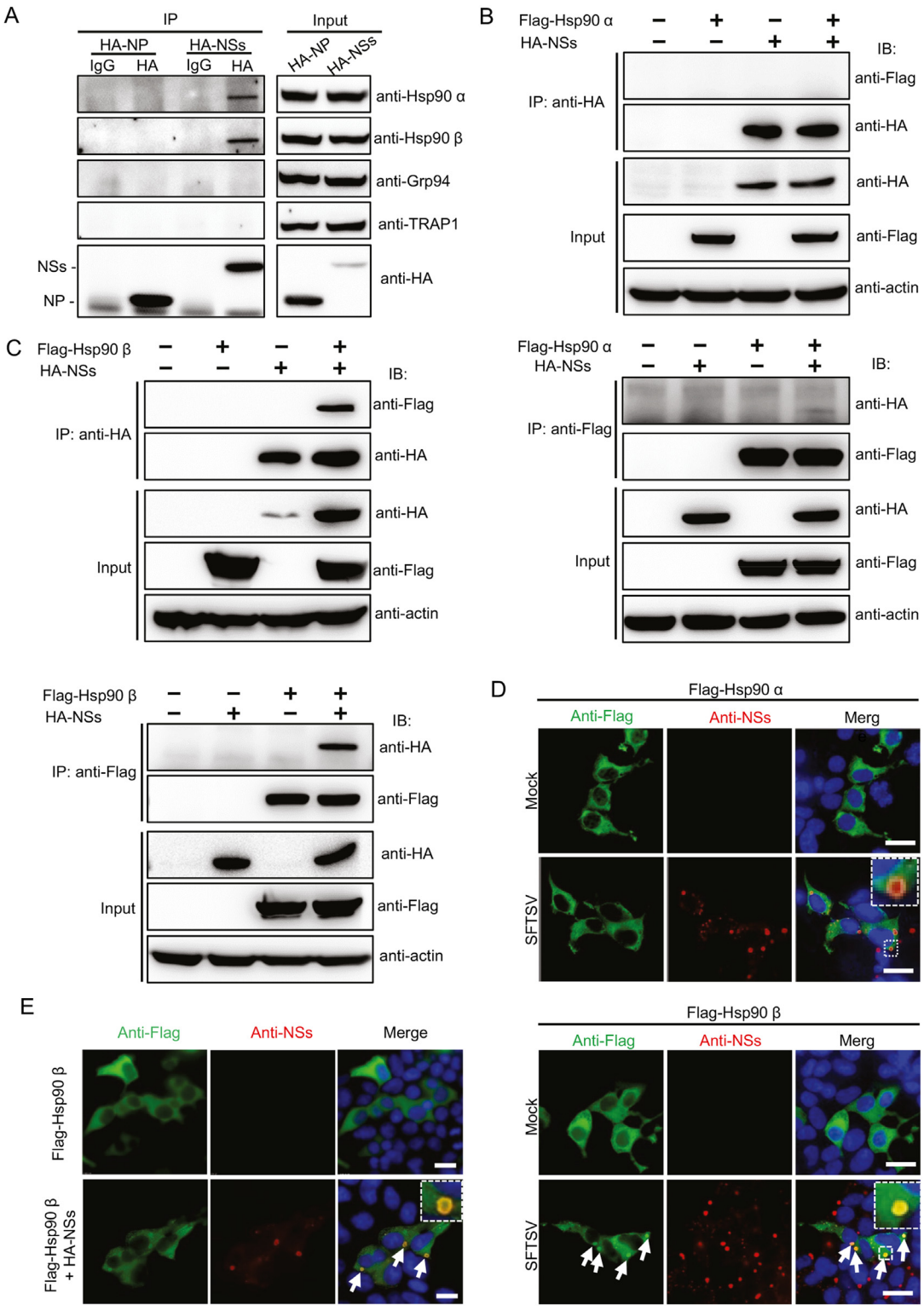

Fig. 5. Hsp90 β interacts with NSs of SFTSV. **A** Co-immunoprecipitation (Co-IP) results of NSs with endogenous Hsp90 isomers. HEK293T cells were transfected with plasmids expressing HA-NP or HA-NSs. After 48 h, cells were lysed for Co-IP analysis with hemagglutinin (HA) antibodies or mouse IgG (control). The immunoprecipitated or input proteins were analyzed using Western blotting with anti-HA, anti-Hsp90 α1, anti-Hsp90 β, anti-GRP94, or anti-TRAP1 antibodies. The protein bands are indicated. (**B, C**) NSs interact with exogenous Hsp90 β. HEK293T cells were transfected or co-transfected with plasmids expressing HA-NSs, Flag-HSP90α, and Flag-HSP90β as indicated. After 48 h, cells were lysed for Co-IP analysis with anti-HA or anti-Flag antibodies. The input and immunoprecipitated samples were immunoblotted with indicated antibodies. (**D, E**) Hsp90 β colocalized with NSs. **D** HEK293 cells transfected with plasmids expressing Flag-Hsp90 α (upper panel) or Flag-Hsp90 β (lower panel) were super-infected with SFTSV at 24 h post-transfection. **E** HEK293 cells transfected with plasmids expressing Flag-Hsp90 β with or without HA-NSs. At 24 h post-infection/transfection, cells were immunostained with anti-Flag (mouse-derived) and anti-NSs (rabbit-derived) antibodies, followed by staining with AF488-conjugated anti-mouse IgG and AF594-conjugated anti-rabbit IgG, respectively. Cell nuclei were stained with DAPI. The small image in the upper right corner is the enlarged image of box region in (**D**) and (**E**). Scale bars, 20 μm (**D**) or 50 μm (**E**).

blotting analysis showed that recombinant NSs were affected in a similar manner to virally-produced NSs by 17-AAG and CHX. Therefore, 17-AAG likely affected the protein synthesis of NSs.

3.5. *Hsp90 β interacts with nonstructural proteins of severe fever with thrombocytopenia syndrome virus*

In human cells, there are mainly four isoforms of Hsp90: Hsp90 α, Hsp90 β, GRP94, and TRAP1. All isomers contain an N-terminal domain responsible for ATP binding, a middle domain important for client binding, and a C-terminal domain responsible for dimerization. The interaction between NSs and endogenous Hsp90 isoforms was determined using Co-IP. HEK293 cells were transfected with plasmids expressing HA-tagged NSs (HA-NSs) and immunoprecipitated with HA antibody or mouse IgG. Cells transfected with plasmids expressing HA-tagged NP (HA-NP) were used as controls. Immunoprecipitated and input proteins were analyzed using Western blotting with anti-Hsp90 α, anti-Hsp90 β, anti-GRP94, anti-TRAP1, and anti-HA antibodies. As shown in Fig. 5A, among the four endogenous Hsp90 isomers, Hsp90 α and β were precipitated by anti-HA antibodies from the cells transfected with HA-NSs, whereas mouse IgG could not precipitate any of the Hsp90 isomers. Neither anti-HA nor mouse IgG could precipitate the Hsp90 isomers in cells transfected with HA-NP. These results indicate that Hsp90 α and β might interact with NSs and were thus selected for further analysis.

As Hsp90 α and β are highly homologous with 85% amino acid sequence identity and functionally overlap in the cytoplasm (Hoter et al., 2018), we further distinguished their interactions with NSs. HEK293T cells were co-transfected with plasmids expressing HA-NSs and Flag-Hsp90 α or Flag-Hsp90 β, and then a Co-IP assay was performed with anti-HA or anti-Flag antibodies, respectively. As shown in Fig. 5B and C, Hsp90 β (Fig. 5C, upper panel), rather than Hsp90 α (Fig. 5B, upper panel), was precipitated during Co-IP using an anti-HA antibody. Consistently, when an anti-Flag antibody was used for Co-IP, NSs were detected in the samples co-transfected with plasmids expressing Flag-Hsp90 β (Fig. 5C, lower panel), but not in those with Flag-Hsp90 α (Fig. 5B, lower panel). These results suggest that Hsp90 β, rather than Hsp90 α, interacts with NSs.

To further validate the interaction between NSs and Hsp90 α/β, immunofluorescence analysis was conducted using HEK293 cells over-expressing Flag-Hsp90 α or Flag-Hsp90 β, and super-infected with SFTSV (Fig. 5D). In the control without SFTSV infection (Mock), Hsp90 α and β were diffusely distributed in the cytoplasm of transfected cells and no

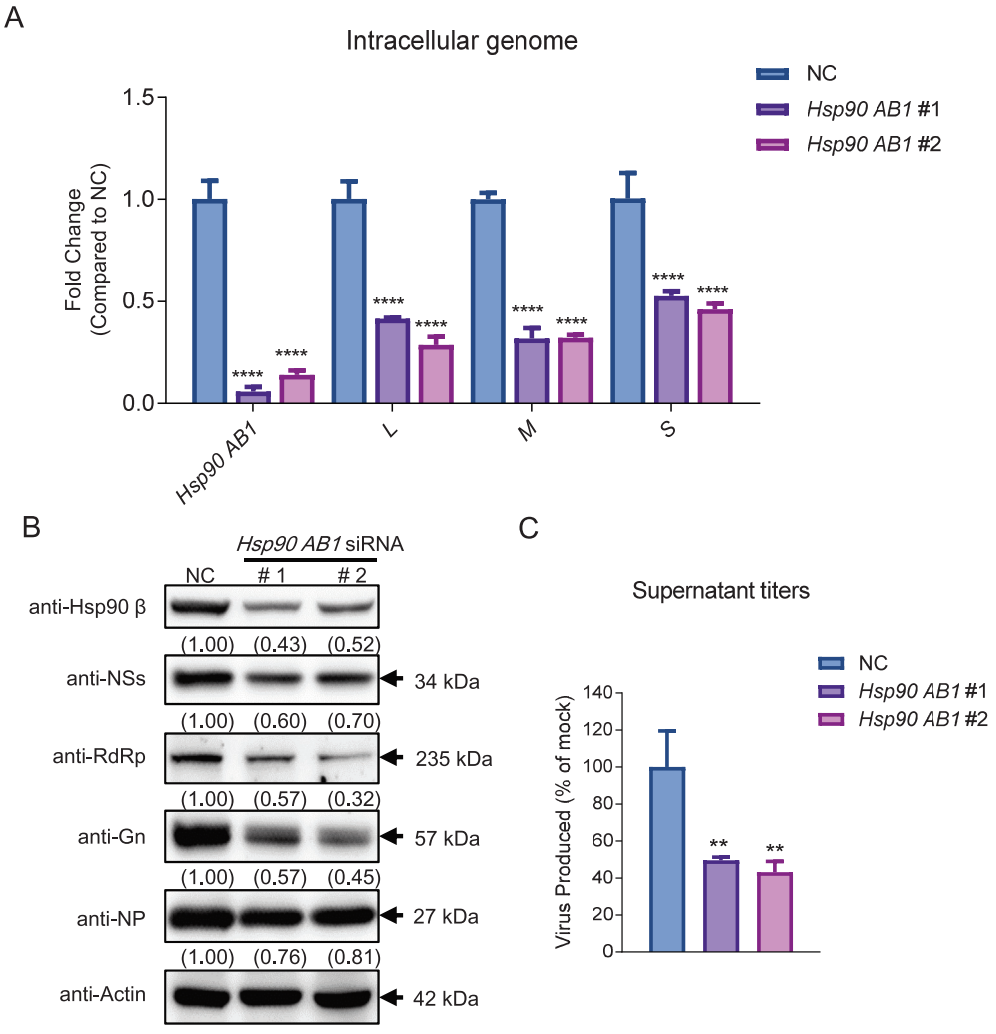

Fig. 6. Knockdown of Hsp90 β influences SFTSV replication. HEK293 cells were transfected with HSP90AB1-derived siRNA. After 48 h, cells were infected with SFTSV at an MOI of 1 for an additional 48 h. The levels of intracellular viral genome were quantified using quantitative real-time PCR (**A**), expression of viral proteins detected through immunoblotting (**B**), and titers in supernatant determined using an endpoint dilution assay and normalized to NC (**C**). NC, negative control. For analysis of the viral production and genome replication, three in-dependent experiments were performed. For detection of viral protein expression, two in-dependent experiments were performed, and representative immunoblot results are shown in the figure. Data are shown as the mean ± SD. Statistical significance was determined using two-way (**A**) or one-way ANOVA (**C**) followed by Dunnett's multiple comparisons test. **, $P < 0.01$; and ****, $P < 0.0001$.

inclusion bodies formed (Fig. 5D). However, in SFTSV-infected cells, Hsp90 β could form spot-like aggregates in the cytoplasm (white arrows in the "Anti-Flag" field), and obviously colocalized with the NS-induced inclusion bodies (white arrows in the "Merge" field) (Fig. 5D, lower panel). In SFTSV-infected cells, Hsp90 α was still dispersed in the cytoplasm (Fig. 5D, upper panel). Furthermore, the direct interaction between Hsp90 β and NSs was also confirmed by overexpression of Hsp90 β and NSs by plasmids (Fig. 5E). These results demonstrate that NSs mainly interact with Hsp90 β in the cytoplasm.

3.6. Knockdown of Hsp90 β influences severe fever with thrombocytopenia syndrome virus infection

To examine whether the suppression of Hsp90 β could influence SFTSV infection, we used siRNA to knockdown Hsp90 β. Hsp90 β is encoded by the *HSP90AB1* gene and two specific siRNAs (Hsp90 AB1#1 and Hsp90 AB1#2) were designed and transfected into HEK293 cells. Both siRNAs significantly knocked down the transcription of Hsp90 β and dramatically suppressed replication of the three viral genome segments (Fig. 6A). Consistently, both siRNAs markedly reduced the protein expression level of Hsp90 β, as well as that of the viral NSs, RdRp, Gn, and NP (Fig. 6 B). In addition, the production of SFTSV virion progeny in the supernatant was significantly decreased by the siRNAs (Fig. 6C). Taken together, Hsp90 β knockdown significantly reduced SFTSV replication.

4. Discussion

In this study, we showed that Hsp90 inhibitors significantly reduced replication and viral protein expression of SFTSV. Further analyses showed that Hsp90 inhibitors specifically affected the protein synthesis of NSs and formation of inclusion bodies. Among the four isoforms of Hsp90, Hsp90 β specifically interacted with NSs, and its knockdown also affected SFTSV infection and the formation of NSs inclusion bodies.

SFTSV NSs have the unique property of forming cytoplasmic inclusion bodies, in which NSs entrap several host factors of the IFN pathway and block their function. For example, NSs sequester TBK1, IKKε, and IRF-3 into the viral inclusion body, thus blocking IFN-β production (Qu et al., 2012; Wu et al., 2014b). They also interact with IRF-7 and suppress the production of IRF7-mediated IFN-α2 and IFN-α4 (Hong et al., 2019). Moreover, NSs entrap the E3 ubiquitin ligase, TRIM25, and thus hinder TRIM25-mediated ubiquitination, the activation of RIG-I, and production of IFN (Min et al., 2020). STAT2 is also entrapped in NSs-induced inclusion bodies, thus further inhibiting IFN-induced antiviral response by blocking type I IFN-stimulated JAK-STAT signaling (Ning et al., 2015; Kitagawa et al., 2018; Yoshikawa et al., 2019). Overall, NSs are strong inhibitors of the host innate immune response. It has also been hypothesized that SFTSV NSs inclusion bodies might be directly involved in viral RNA replication by acting as replication platforms (Wu et al., 2014a; Sun et al., 2016). Our results showed that Hsp90 inhibitors can block the formation of NSs inclusion bodies; therefore, we speculated that the disruption of NSs inclusion bodies could be a key working mechanism of Hsp90 inhibitors against SFTSV infection, which weakens the ability of NSs to antagonize the host's antiviral responses and disrupt the viral replication platform.

In the absence of Hsp90, its client proteins are degraded via the proteasomal or autophagy pathways (Wang et al., 2017). For example, 17-DMAG induced degradation of the Tax protein of human T-cell virus mainly through the proteasome pathway, and this degradation can be reversed by the proteasome inhibitor, MG-132 (Gao and Harhaj, 2013). During EBV infection, the autophagy inhibitor, 3-MA, partially increased EBV protein kinase expression levels in the presence of 17-DMAG (Sun et al., 2013). However, in our study, both autophagy and proteasomal inhibitors could not reverse the decrease in expression of SFTSV NSs caused by 17-AAG treatment (Fig. 3), and the change in NSs protein level patterns caused by 17-AAG exposure was similar to that induced by the protein synthesis inhibitor, CHX (Fig. 3). These results collectively indicated that Hsp90 inhibitors did not affect the stability of NSs but might block their translation. Notably, Hsp90 inhibitors have been shown to decrease the synthesis of various viral proteins, including EBV nuclear antigen 1 (EBNA1) and HCMV UL97 kinases (Sun et al., 2010; Sun et al., 2013). As an important molecular chaperone, Hsp90 cooperates with other chaperones, such as Hsp60 and Hsp70, which play important roles in the co-translational folding process of newly synthesized polypeptide chains (Kramer et al., 2009). The specific mechanism by which Hsp90 is involved in NSs expression requires further investigation.

The decrease in NSs expression levels may directly result in the interruption of NSs inclusion body formation caused by Hsp90 inhibitors. In additions, since Hsp90 members are important chaperones, they may be required for the assembly of NSs inclusion bodies. Currently, the mechanism by which NSs assemble into inclusion bodies remains unclear. It would be interesting to further investigate the role of Hsp90 β during NSs inclusion body assembly.

Hsp90 members are involved in multiple processes related to cell function and viral infection. Although our data suggested that NSs may be the main client protein of Hsp90 β, we cannot exclude the possibility that other viral or cellular proteins are affected by Hsp90 during SFTSV infection. Nevertheless, our results clearly showed that Hsp90 inhibition could significantly affect SFTSV infection and NSs inclusion body formation. This information is helpful for further understanding the virus-host interactions of SFTSV and the development of antiviral drugs.

5. Conclusions

We demonstrated that Hsp90 inhibitors could significantly inhibit the SFTSV infection, and markedly decreased the expression of the SFTSV-encoded main virulence factor, NSs, in SFTSV infected cells. Interestingly, our results suggest that, rather than decreasing the stability of NSs, Hsp90 inhibitors mainly reduced the translation of NSs. Among the four isoforms, the cytoplasmic isoform Hsp90 β associated with NSs, and knocking down the expression of Hsp90 β also inhibited the replication of SFTSV. This study provides new insight into the regulation of NSs expression by host factors and also suggests that Hsp90 inhibitors may exert therapeutic benefits for SFTS disease.

Data availability

All data generated or analyzed during the current study are included in this manuscript.

Ethics statement

This article does not contain any studies with human and animal subjects performed by any of the authors.

Author contributions

Bo wang: investigation and data curation. Leike Zhang: conceptualization. Fei Deng: resources. Zhihong Hu: conceptualization, writing-review&editing. Manli Wang: conceptualization, methodology, and writing-review&editing. Jia Liu: investigation, data curation, writing-original draft. All authors have read and agreed to the version of the manuscript.

Conflict of interest

The authors declare that they have no conflict of interest. Prof. Fei Deng is an editorial board member for Virologica Sinica and was not involved in the editorial review or the decision to publish this article.

Acknowledgments

We thank Prof. Wuchun Cao from State Key Laboratory of Pathogen and Biosecurity, Beijing Institute of Microbiology and Epidemiology for

providing SFTSV WCH-2011/HN/China/isolate 97. We thank for Dr. Ding Gao from the core faculty of Wuhan Institute of Virology for their critical support. This work was supported by grants from the National Natural Science Foundation of China (31900146), the key Biosafety Science and Technology Program of Hubei Jiangxia Laboratory (JXBS001), the Hubei Natural Science Foundation for Distinguished Young Scholars (2021CFA050), and the Creative Research Group Program of Natural Science Foundation of Hubei Province (2022CFA021).

Appendix A. Supplementary data

Supplementary data to this article can be found online at https://doi.org/10.1016/j.virs.2023.11.008.

References

Abudurexiti, A., Adkins, S., Alioto, D., Alkhovsky, S.V., Avšič-Županc, T., Ballinger, M.J., Bente, D.A., Beer, M., Bergeron, É., Blair, C.D., Briese, T., Buchmeier, M.J., Burt, F.J., Calisher, C.H., Cháng, C., Charrel, R.N., Choi, I.R., Clegg, J.C.S., De La Torre, J.C., De Lamballerie, X., Dèng, F., Di Serio, F., Digiaro, M., Drebot, M.A., Duàn, X., Ebihara, H., Elbeaino, T., Ergünay, K., Fulhorst, C.F., Garrison, A.R., Gāo, G.F., Gonzalez, J.J., Groschup, M.H., Günther, S., Haenni, A.L., Hall, R.A., Hepojoki, J., Hewson, R., Hú, Z., Hughes, H.R., Jonson, M.G., Junglen, S., Klempa, B., Klingström, J., Kòu, C., Laenen, L., Lambert, A.J., Langevin, S.A., Liu, D., Lukashevich, I.S., Luò, T., Lǚ, C., Maes, P., De Souza, W.M., Marklewitz, M., Martelli, G.P., Matsuno, K., Mielke-Ehret, N., Minutolo, M., Mirazimi, A., Moming, A., Mühlbach, H.P., Naidu, R., Navarro, B., Nunes, M.R.T., Palacios, G., Papa, A., Pauvolid-Corrêa, A., Pawęska, J.T., Qiáo, J., Radoshitzky, S.R., Resende, R.O., Romanowski, V., Sall, A.A., Salvato, M.S., Sasaya, T., Shěn, S., Shí, X., Shirako, Y., Simmonds, P., Sironi, M., Song, J.W., Spengler, J.R., Stenglein, M.D., Sū, Z., Sūn, S., Táng, S., Turina, M., Wáng, B., Wáng, C., Wáng, H., Wáng, J., Wèi, T., Whitfield, A.E., Zerbini, F.M., Zhāng, J., Zhāng, L., Zhāng, Y., Zhang, Y.Z., Zhāng, Y., Zhou, X., Zhū, L., Kuhn, J.H., 2019. Taxonomy of the order Bunyavirales: update 2019. Arch. Virol. 164, 1949–1965.

Albornoz, A., Hoffmann, A.B., Lozach, P.Y., Tischler, N.D., 2016. Early bunyavirus-host cell interactions. Viruses 8, 143.

Basta, S., Stoessel, R., Basler, M., Van Den Broek, M., Groettrup, M., 2005. Cross-presentation of the long-lived lymphocytic choriomeningitis virus nucleoprotein does not require neosynthesis and is enhanced via heat shock proteins. J. Immunol. 175, 796–805.

Burch, A.D., Weller, S.K., 2005. Herpes simplex virus type 1 DNA polymerase requires the mammalian chaperone hsp90 for proper localization to the nucleus. J. Virol. 79, 10740–10749.

Chen, B., Piel, W.H., Gui, L., Bruford, E., Monteiro, A., 2005. The HSP90 family of genes in the human genome: insights into their divergence and evolution. Genomics 86, 627–637.

Chen, W., Sin, S.H., Wen, K.W., Damania, B., Dittmer, D.P., 2012. Hsp90 inhibitors are efficacious against Kaposi Sarcoma by enhancing the degradation of the essential viral gene LANA, of the viral co-receptor EphA2 as well as other client proteins. PLoS Pathog. 8, e1003048.

Choi, Y., Park, S.J., Sun, Y., Yoo, J.S., Pudupakam, R.S., Foo, S.S., Shin, W.J., Chen, S.B., Tsichlis, P.N., Lee, W.J., Lee, J.S., Li, W., Brennan, B., Choi, Y.K., Jung, J.U., 2019. Severe fever with thrombocytopenia syndrome phlebovirus non-structural protein activates TPL2 signalling pathway for viral immunopathogenesis. Nat Microbiol 4, 429–437.

Gao, L., Harhaj, E.W., 2013. HSP90 protects the human T-cell leukemia virus type 1 (HTLV-1) tax oncoprotein from proteasomal degradation to support NF-kappaB activation and HTLV-1 replication. J. Virol. 87, 13640–13654.

Gu, X.L., Su, W.Q., Zhou, C.M., Fang, L.Z., Zhu, K., Ma, D.Q., Jiang, F.C., Li, Z.M., Li, D., Duan, S.H., Peng, Q.M., Wang, R., Jiang, Y., Han, H.J., Yu, X.J., 2022. SFTSV infection in rodents and their ectoparasitic chiggers. PLoS Neglected Trop. Dis. 16, e0010698.

Hong, Y., Bai, M., Qi, X., Li, C., Liang, M., Li, D., Cardona, C.J., Xing, Z., 2019. Suppression of the IFN-α and -β induction through sequestering IRF7 into viral inclusion bodies by nonstructural protein NSs in severe fever with thrombocytopenia syndrome bunyavirus infection. J. Immunol. 202, 841–856.

Hoter, A., El-Sabban, M.E., Naim, H.Y., 2018. The HSP90 family: structure, regulation, function, and implications in health and disease. Int. J. Mol. Sci. 19, 2560.

Khalil, J., Kato, H., Fujita, T., 2021. The role of non-structural protein NSs in the pathogenesis of severe fever with thrombocytopenia syndrome. Viruses 13, 876.

Kitagawa, Y., Sakai, M., Shimojima, M., Saijo, M., Itoh, M., Gotoh, B., 2018. Nonstructural protein of severe fever with thrombocytopenia syndrome phlebovirus targets STAT2 and not STAT1 to inhibit type I interferon-stimulated JAK-STAT signaling. Microb. Infect. 20, 360–368.

Kramer, G., Boehringer, D., Ban, N., Bukau, B., 2009. The ribosome as a platform for co-translational processing, folding and targeting of newly synthesized proteins. Nat. Struct. Mol. Biol. 16, 589–597.

Lam, T.T., Liu, W., Bowden, T.A., Cui, N., Zhuang, L., Liu, K., Zhang, Y.Y., Cao, W.C., Pybus, O.G., 2013. Evolutionary and molecular analysis of the emergent severe fever with thrombocytopenia syndrome virus. Epidemics 5, 1–10.

Liu, Y., Li, Q., Hu, W., Wu, J., Wang, Y., Mei, L., Walker, D.H., Ren, J., Wang, Y., Yu, X.J., 2012. Person-to-person transmission of severe fever with thrombocytopenia syndrome virus. Vector Borne Zoonotic Dis. 12, 156–160.

Min, Y.Q., Ning, Y.J., Wang, H., Deng, F., 2020. A RIG-I-like receptor directs antiviral responses to a bunyavirus and is antagonized by virus-induced blockade of TRIM25-mediated ubiquitination. J. Biol. Chem. 295, 9691–9711.

Naito, T., Momose, F., Kawaguchi, A., Nagata, K., 2007. Involvement of Hsp90 in assembly and nuclear import of influenza virus RNA polymerase subunits. J. Virol. 81, 1339–1349.

Ning, Y.J., Feng, K., Min, Y.Q., Cao, W.C., Wang, M., Deng, F., Hu, Z., Wang, H., 2015. Disruption of type I interferon signaling by the nonstructural protein of severe fever with thrombocytopenia syndrome virus via the hijacking of STAT2 and STAT1 into inclusion bodies. J. Virol. 89, 4227–4236.

Qu, B., Qi, X., Wu, X., Liang, M., Li, C., Cardona, C.J., Xu, W., Tang, F., Li, Z., Wu, B., Powell, K., Wegner, M., Li, D., Xing, Z., 2012. Suppression of the interferon and NF-kappaB responses by severe fever with thrombocytopenia syndrome virus. J. Virol. 86, 8388–8401.

Reyes-Del Valle, J., Chávez-Salinas, S., Medina, F., Del Angel, R.M., 2005. Heat shock protein 90 and heat shock protein 70 are components of dengue virus receptor complex in human cells. J. Virol. 79, 4557–4567.

Rochlin, I., Benach, J.L., Furie, M.B., Thanassi, D.G., Kim, H.K., 2022. Rapid invasion and expansion of the Asian longhorned tick (Haemaphysalis longicornis) into a new area on Long Island, New York, USA. Ticks Tick Borne Dis 14, 102088.

Solit, D.B., Chiosis, G., 2008. Development and application of Hsp90 inhibitors. Drug Discov. Today 13, 38–43.

Song, P., Zheng, N., Liu, Y., Tian, C., Wu, X., Ma, X., Chen, D., Zou, X., Wang, G., Wang, H., Zhang, Y., Lu, S., Wu, C., Wu, Z., 2018. Deficient humoral responses and disrupted B-cell immunity are associated with fatal SFTSV infection. Nat. Commun. 9, 3328.

Sun, Q., Qi, X., Zhang, Y., Wu, X., Liang, M., Li, C., Li, D., Cardona, C.J., Xing, Z., 2016. Synaptogyrin-2 promotes replication of a novel tick-borne bunyavirus through interacting with viral nonstructural protein NSs. J. Biol. Chem. 291, 16138–16149.

Sun, X., Barlow, E.A., Ma, S., Hagemeier, S.R., Duellman, S.J., Burgess, R.R., Tellam, J., Khanna, R., Kenney, S.C., 2010. Hsp90 inhibitors block outgrowth of EBV-infected malignant cells in vitro and in vivo through an EBNA1-dependent mechanism. Proc. Natl. Acad. Sci. U.S.A. 107, 3146–3151.

Sun, X., Bristol, J.A., Iwahori, S., Hagemeier, S.R., Meng, Q., Barlow, E.A., Fingeroth, J.D., Tarakanova, V.L., Kalejta, R.F., Kenney, S.C., 2013. Hsp90 inhibitor 17-DMAG decreases expression of conserved herpesvirus protein kinases and reduces virus production in Epstein-Barr virus-infected cells. J. Virol. 87, 10126–10138.

Tsou, Y.L., Lin, Y.W., Chang, H.W., Lin, H.Y., Shao, H.Y., Yu, S.L., Liu, C.C., Chitra, E., Sia, C., Chow, Y.H., 2013. Heat shock protein 90: role in enterovirus 71 entry and assembly and potential target for therapy. PLoS One 8, e77133.

Tufts, D.M., Goodman, L.B., Benedict, M.C., Davis, A.D., Vanacker, M.C., Diuk-Wasser, M., 2021. Association of the invasive Haemaphysalis longicornis tick with vertebrate hosts, other native tick vectors, and tick-borne pathogens in New York City, USA. Int. J. Parasitol. 51, 149–157.

Wang, Y., Jin, F., Wang, R., Li, F., Wu, Y., Kitazato, K., Wang, Y., 2017. HSP90: a promising broad-spectrum antiviral drug target. Arch. Virol. 162, 3269–3282.

Wu, X., Qi, X., Liang, M., Li, C., Cardona, C.J., Li, D., Xing, Z., 2014a. Roles of viroplasm-like structures formed by nonstructural protein NSs in infection with severe fever with thrombocytopenia syndrome virus. Faseb. J. 28, 2504–2516.

Wu, X., Qi, X., Qu, B., Zhang, Z., Liang, M., Li, C., Cardona, C.J., Li, D., Xing, Z., 2014b. Evasion of antiviral immunity through sequestering of TBK1/IKKε/IRF3 into viral inclusion bodies. J. Virol. 88, 3067–3076.

Yang, K., Shi, H., Qi, R., Sun, S., Tang, Y., Zhang, B., Wang, C., 2006. Hsp90 regulates activation of interferon regulatory factor 3 and TBK-1 stabilization in Sendai virus-infected cells. Mol. Biol. Cell 17, 1461–1471.

Yoshikawa, R., Sakabe, S., Urata, S., Yasuda, J., 2019. Species-specific pathogenicity of severe fever with thrombocytopenia syndrome virus is determined by anti-STAT2 activity of NSs. J. Virol. 93.

Yu, X.J., Liang, M.F., Zhang, S.Y., Liu, Y., Li, J.D., Sun, Y.L., Zhang, L., Zhang, Q.F., Popov, V.L., Li, C., Qu, J., Li, Q., Zhang, Y.P., Hai, R., Wu, W., Wang, Q., Zhan, F.X., Wang, X.J., Kan, B., Wang, S.W., Wan, K.L., Jing, H.Q., Lu, J.X., Yin, W.W., Zhou, H., Guan, X.H., Liu, J.F., Bi, Z.Q., Liu, G.H., Ren, J., Wang, H., Zhao, Z., Song, J.D., He, J.R., Wan, T., Zhang, J.S., Fu, X.P., Sun, L.N., Dong, X.P., Feng, Z.J., Yang, W.Z., Hong, T., Zhang, Y., Walker, D.H., Wang, Y., Li, D.X., 2011. Fever with thrombocytopenia associated with a novel bunyavirus in China. N. Engl. J. Med. 364, 1523–1532.

Zhang, J., Li, H., Liu, Y., Zhao, K., Wei, S., Sugarman, E.T., Liu, L., Zhang, G., 2022. Targeting HSP90 as a novel therapy for cancer: mechanistic insights and translational relevance. Cells 11, 2778.

Zhang, L.K., Wang, B., Xin, Q., Shang, W., Shen, S., Xiao, G., Deng, F., Wang, H., Hu, Z., Wang, M., 2019. Quantitative proteomic analysis reveals unfolded-protein response involved in severe fever with thrombocytopenia syndrome virus infection. J. Virol. 93.